10-1-2016

# Large-scale screening of preferred interactions of human src homology-3 (SH3) domains using native target proteins as affinity ligands

Arunas Kazlauskas
*Helsingin Yliopisto*

Constanze Schmotz
*Helsingin Yliopisto*

Tapio Kesti
*Helsingin Yliopisto*

Jussi Hepojoki
*Helsingin Yliopisto*

Iivari Kleino
*Helsingin Yliopisto*

*See next page for additional authors*

Citation of this paper:

Kazlauskas, Arunas; Schmotz, Constanze; Kesti, Tapio; Hepojoki, Jussi; Kleino, Iivari; Kaneko, Tomonori; Li, Shawn S.C.; Saksela, Kalle; Yusifov; Skarina, Tatiana; Evdokimova, Elena; Ackloo, Suzanne; Lowes, Lori; Hedley, Benjamin D.; Bhayana, Vipin; Chin-Yee, Ian; and Li, Shawn S.C., "Large-scale screening of preferred interactions of human src homology-3 (SH3) domains using native target proteins as affinity ligands" (2016). *Paediatrics Publications*. 2133.
https://ir.lib.uwo.ca/paedpub/2133

## Authors

Arunas Kazlauskas, Constanze Schmotz, Tapio Kesti, Jussi Hepojoki, Iivari Kleino, Tomonori Kaneko, Shawn S.C. Li, Kalle Saksela, Yusifov, Tatiana Skarina, Elena Evdokimova, Suzanne Ackloo, Lori Lowes, Benjamin D. Hedley, Vipin Bhayana, Ian Chin-Yee, and Shawn S.C. Li

# Large-Scale Screening of Preferred Interactions of Human Src Homology-3 (SH3) Domains Using Native Target Proteins as Affinity Ligands*⒮

Arunas Kazlauskas‡‖**, Constanze Schmotz‡‖, Tapio Kesti‡, Jussi Hepojoki‡, Iivari Kleino‡, Tomonori Kaneko§, Shawn S.C. Li§, and Kalle Saksela‡¶

The Src Homology-3 (SH3) domains are ubiquitous protein modules that mediate important intracellular protein interactions via binding to short proline-rich consensus motifs in their target proteins. The affinity and specificity of such core SH3 - ligand contacts are typically modest, but additional binding interfaces can give rise to stronger and more specific SH3-mediated interactions. To understand how commonly such robust SH3 interactions occur in the human protein interactome, and to identify these in an unbiased manner we have expressed 324 predicted human SH3 ligands as full-length proteins in mammalian cells, and screened for their preferred SH3 partners using a phage display-based approach. This discovery platform contains an essentially complete repertoire of the ~300 human SH3 domains, and involves an inherent binding threshold that ensures selective identification of only SH3 interactions with relatively high affinity. Such strong and selective SH3 partners could be identified for only 19 of these 324 predicted ligand proteins, suggesting that the majority of human SH3 interactions are relatively weak, and thereby have capacity for only modest inherent selectivity. The panel of exceptionally robust SH3 interactions identified here provides a rich source of leads and hypotheses for further studies. However, a truly comprehensive characterization of the human SH3 interactome will require novel high-throughput methods based on function instead of absolute binding affinity. *Molecular & Cellular Proteomics 15: 10.1074/mcp.M116.060483, 3270–3281, 2016.*

The Src Homology-3 (SH3)[1] domain is one of the most common modular domains in eukaryotic genomes. SH3 domains serve to guide interaction of proteins that typically are involved in regulation of cell growth and differentiation, and are often involved in pathogenesis of diseases such as cancer (1–3). In addition, microbial pathogens, such as HIV, can exploit SH3-mediated cellular processes (4–6). Human proteome contains ~300 different SH3 domains and many more SH3 ligand proteins, creating an enormous number of theoretically possible SH3 interactions. Knowing which particular of these interactions actually take place and are biologically meaningful would greatly increase our understanding about the signaling networks that regulate normal cellular behavior and become deregulated in many important diseases.

SH3 domains are relatively short (~60 residues) modules that are specialized in binding to proline-rich target peptides (7–9). These peptides typically contain a PxxP core-binding motif (where x is any amino acid) flanked by a basic residue on either side of the PxxP motif, but a large number and variety of unconventional SH3 target motifs have also been identified (9). A shallow groove on the surface of SH3 domains formed by a set of conserved hydrophobic residues is adapted to bind to these target peptides. Additional contacts between variable SH3 loop regions and ligand residues outside of the PxxP motif can be critical in determining the specificity and affinity of binding. The capacity of such complex molecular interactions to contribute to the strength and selectivity of SH3 binding has been highlighted by structural and biochemical studies on recruitment of the SH3 domain of the tyrosine kinase Hck by the HIV-1 pathogenicity factor Nef (10, 11). However, it is unclear how common such strong and specific SH3 binding is in nature. In other words, it is not known how many of all SH3/ligand complexes involved in guiding of eukaryotic protein interactions actually play a dominant role in defining these partnerships. Indeed, it can be envisioned that in many cases SH3-target peptide contacts play more subtle

---

[1] The abbreviations used are: SH3, Src Homology-3; ROS, reactive oxygen species; PPI, protein-protein interaction; cfu, colony forming units; Y2H, yeast two-hybrid.

roles in coordinating the architecture of protein complexes, and despite being important for cellular regulation do not need to involve high binding affinities or great inherent selectivity.

We have developed an experimental platform for unbiased and comprehensive identification of preferred interactions between SH3 domains and their ligand proteins. This approach is based on the use of a phage-display library containing a virtually complete collection of human SH3 domains ($n = 296$) (12). This system allows an unbiased identification of the SH3 domains that show preferential binding to ligand proteins of interests. Because these target proteins are expressed in their native form, this system has the potential to explore binding affinity and specificity contributed by contacts provided by the peptide binding interface, as well as more complex and atypical interactions. The binding affinity required for positive identification of a specific interaction in this discovery system is relatively high (estimated to be in the range of 2 to 5 $\mu$M), as interactions with dissociation constants higher than 5 $\mu$M are rarely found (12–25) and unpublished observations). Although this may be seen as a technical limitation when considering that many SH3 interactions with established roles in cell biology are weak such an affinity threshold is also a major experimental advantage by filtering out nonspecific background caused by promiscuous low affinity binding that most SH3 domains exhibit toward a variety of proline-rich sequences. The possibility to use native SH3 ligand proteins as "baits," and the capacity to interrogate the complete SH3 repertoire in parallel, combined with the virtually complete lack of confounding variables unrelated to binding affinity provide this approach with distinct advantages over other experimental systems, such as yeast two-hybrid (Y2H) and peptide array screening that have been actively used to decipher SH3 mediated protein interaction networks (26–33).

Our earlier work on a variety of individual ligand proteins of interest has established the value of this phage library in identifying SH3-mediated interactions that involve distinct affinity and selectivity (12–22). In this study we apply recombination-mediated cloning for expression of hundreds of potential SH3 ligand proteins in cultured human cells to identify preferred SH3-mediated interactions among the human proteome in a high throughput manner.

EXPERIMENTAL PROCEDURES

*Generation of Expression Vectors Encoding Potential SH3 Ligand Proteins*—The 449 open reading frames (ORFs) of potential SH3 ligand proteins have been obtained from the Human ORFeome v3.1 library (34) as Gateway recombination-compatible entry constructs (35) encoding full-length cDNA sequences of ORFs flanked by *att*L1 and *att*L2 sites required for site-specific recombination of the entry clone with a Gateway destination vector. The Gateway-compatible destination vector pEBB/PP-DEST has been generated by subcloning a fragment from the modified pDEST vector (a kind gift from Jussi Taipale, University of Helsinki, Finland), which encodes chloramphenicol resistance and *ccd*B genes flanked by recombination sites *att*R1 and *att*R2 into pEBB/PP vector (please contact authors for cloning

details of this construct). The pEBB/PP vector is driven by the elongation factor 1$\alpha$ (EF-1$\alpha$) promoter, and contains a 123 amino acids long biotin acceptor domain (19), to which we will refer as the "PP domain" in the presented study. Recombination (Gateway LR) reactions between pEBB/PP-DEST and individual ORFs were performed by using Gateway LR Clonase II Enzyme Mix (Invitrogen, Carlsbad, CA) according to manufacturer's recommendations. Each of the resultant pEBB/PP-ORF constructs encoded the desired ORF in frame with PP domain sequence at the N terminus.

*Protein Expressions and Streptavidin Coprecipitations*—293FT cells were transfected by standard calcium phosphate precipitation method with pEBB/PP-ORF expression vectors or empty pEBB/PP vector alone (control samples) corresponding to a total of 10–16 $\mu$g of plasmid DNA per 10 cm culture dish. After 36 h of transfection, cells were collected in PBG buffer (1$\times$ phosphate buffered saline (PBS) supplemented with 10% glycerol and 0.5% Tween-20) containing protease inhibitors ("Complete," Roche) and lysed by sonication at 0.2–0.3 kJ on ice by Bandelin Sonoplus homogenizer. 2% aliquots of the unprocessed lysate were used for Western blot analysis, where the IRDye-labeled streptavidin was used for detection of expressed proteins by Odyssey infrared imaging system (LI-COR Biosciences, Lincoln, NE). The rest of the lysates were subjected to precipitation of PP-ORF proteins using streptavidin-coated magnetic beads (Dynabeads M-280-Streptavidin, Invitrogen).

*Phage Display*—Panning of the SH3 phage display library using target proteins was performed as described earlier (12). Briefly, precipitated PP-ligand fusion proteins were incubated with the mixture of human SH3 library-displaying phages ($10^9$–$10^{10}$ colony forming units (cfu) per well), prepared in PBS-T (0.05% Tween-20 in 1$\times$ PBS) and supplemented with 2.5% of nonfat milk, for 2 h at room temperature. The nonbound phages were then removed and the beads were washed four times with 1 ml of PBS-T. Subsequently, phages bound to PP-ligands were incubated with TG1 bacteria (grown to the log-phase of $OD_{600} = 0.5$–0.6) at 37 °C for 1 h followed by seeding of the infected bacteria onto ampicillin-containing lysogeny broth (LB) plates. Ligand-interacting SH3 domains were identified by sequencing of SH3 domain-encoding phagemides (pG8J8/SH3 clones (12) obtained from individual bacterial colonies.

*Peptide Array*—Peptides of interest were synthesized by the Peptide and Protein Laboratory (Haartman Institute, University of Helsinki) as peptide-cellulose conjugates using Multipep (Intavis Bioanalytical Instruments, Cologne, Germany) according to the manufacturer's protocol for SPOT synthesis (36) and printed in parallel arrays on glass slides using SlideSpotter equipment (Intavis Bioanalytical Instruments). The array was immersed for 2 h in Blocking solution (PBS-T supplemented with 5% of nonfat dry milk) followed by washing three times in PBS-T. SH3 domains (Src, Lyn, Fyn, Yes, Tec, Crk, CrkL, CMS (1/3), Amphiphysin (AMPH), BAIAP2L1, ArgBP2, Intersectin 1 (Itsn1) (3/5), Eps8L3) that had been identified as strong binders to at least one of the ligand proteins were expressed in bacteria as glutathione transferase- (GST-) fusions and purified by using affinity chromatography. Individual GST-SH3 domains were diluted with Blocking solution to a final concentration of 1 $\mu$M and incubated with peptide arrays for 2 h at room temperature, followed by three washes with PBS-T and one wash with PBS. The binding was detected with anti-GST antibodies conjugated with the near-fluorescent dye IRDye 800CW (LI-COR Biosciences) and quantified with an Odyssey Infrared Imaging System (LI-COR Biosciences). The binding strength of the SH3 domain for each of the arrayed peptides was estimated according to the obtained fluorescence intensity from the corresponding spot in the array. The binding was rated as selective if the fluorescence signal was higher or about equal to 50% of the highest signal intensity value estimated for the whole array.

*Pull-down Assay*—The SH3 domains were expressed in bacteria as GST-PP domain-fusions and purified as described above. The obtained protein solutions were dialyzed against Nonidet P-40 lysis buffer (150 mM NaCl; 50 mM Tris-HCl, pH 7.4; 1% Nonidet P-40) and adjusted to a final concentration of 0.5 $\mu$M, supplemented with 500 $\mu$M free biotin. An SH3 domain concentration of 0.5 $\mu$M was chosen because it was determined to be optimal for revealing relative differences in the capacity of different ligands proteins to capture different SH3 domains in this setting. The SH3 ligand proteins were expressed in HEK293T cells and immobilized to streptavidin-coated magnetic beads as described above, except that after 1.5 h incubation of the beads and lysates at 4 °C under rotation free biotin was added to a final concentration of 500 $\mu$M to saturate all biotin binding sites on the beads, followed by three washes of the bead-protein complexes with Nonidet P-40 lysis buffer. A bed volume of ~3 $\mu$l of ligand protein-coated beads were added into each Eppendorf tube containing different dilutions of the GST-PP-SH3 proteins in 100 $\mu$l of Nonidet P-40 lysis buffer supplemented with 500 $\mu$M free biotin. This concentration of free biotin was found to be efficient in preventing direct binding of GST-PP-SH3 proteins to beads lacking preimmobilized SH3 ligands. After incubation for 1 h at 4 °C under rotation the beads were washed three times for 30 s with Nonidet P-40 lysis buffer. The proteins associated with the beads after the washes were analyzed by SDS-PAGE and Western blotting using IRDye800CW conjugated streptavidin. Detection was done using the Odyssey infrared imaging system (LI-COR Biosciences). Background reduction and signal quantification were carried out using the Image Studio™Lite Software (LI-COR Biosciences). For Scatchard analysis quantified signals for captured SH3 domains were plotted against the ratio of these signals *versus* the corresponding total concentration of SH3 domain used in the pull-down. $K_D$-values were generated by applying linear regression model on the plotted data, whereas the slope of the regression line corresponds to the negative value of the $K_D$. Total [SH3] was used as an approximation of free [SH3] for Scatchard analyses, which was calculated to be adequate, because the amounts of ligands on the beads were small, and only a minor fraction of total [SH3] was removed from free [SH3] upon ligand binding.

RESULTS

*Phage Display Library-based Screening of the Human SH3 Interactome*—To investigate how commonly distinctly selective and robust SH3 interactions occur in the human interactome, and to identify such interactions in an unbiased manner we set out to make use of our comprehensive SH3 domain library to screen SH3 partners for a large number of potential human SH3 ligand proteins predicted by sequence analysis. As a source of these putative ligand proteins we used a large human cDNA library, Human ORFeome v3.1, which contained 12,212 ORFs, representing 10,214 human genes, in a Gateway-cloning compatible vector backbone (34). The ORFeome v3.1 library database was subjected to a bioinformatic search for predicted SH3 target motifs using algorithms designed to give a high likelihood for the selected ORFs to encode SH3 targets, but without any reference to the existing literature to exclude or include previously reported SH3 interactions.

Two prediction strategies were employed for selection of candidate cDNAs that were subsequently used to express potential ligand proteins for screening of the SH3 library. In the first approach, sequence search parameters were set to identify both the conventional PxxP and unconventional mo-

tifs, such as PxxDY, Px(P/A)xxR, $\Phi$xRPxR, and PxxxRxxKP (where x is any amino acid and $\Phi$ is a hydrophobic residue). We expected that this type of search would identify ligand candidates with high probability of encoding actual SH3 binding proteins. As an alternative approach, we chose ORFs based on the presence of proline- and basic amino acid-rich regions, as well as randomly selected intracellular proteins that had no suggestive SH3 binding motifs, but were involved in cellular signal transduction and contained at least one canonical protein interaction domain (SH3, SH2, or PDZ). We hypothesized that while this second approach would be less likely to identify functional SH3 ligands, it might lead to discovery of novel types of SH3 interactions. By combining these two selection approaches, we identified 449 sequences in the ORFeome v3.1 library database as the SH3 partner candidates for our screening (see supplemental Table S1). Of these proteins 302 contained at least one conventional type I or type II SH3 binding motif, R/Kx$\Phi$PxxP and Px$\Phi$PxR/K, respectively.

The 449 selected ORFs were subjected to subcloning into a Gateway-compatible destination vector pEBB/PP-DEST generated for this purpose (see Experimental Procedures). pEBB/PP-DEST is driven by the elongation factor 1 (EF-1$\alpha$) promoter, and contains a 123 amino acids long biotin acceptor domain ("PP domain"; (19)) plus Gateway destination sequence attR1-ccdB-attR2 for recombination with ORF-encoding sequences and bacterial selection of recombinant clones. The putative ligand proteins were transiently expressed as biotinylated PP-fusion proteins in human embryonic kidney 293T cells (HEK293T), and immobilized onto streptavidin-coated paramagnetic beads for a single round affinity panning of the SH3 phage library. An illustrated outline of this approach is shown in Fig. 1.

As summarized in Table I, 324 ORFs out of the initial 449 clones could be successfully subcloned and expressed as expectedly sized proteins in HEK293T cells (for a complete list, see supplemental Table S1). Expression of PP domain-carrying ORFs was monitored by subjecting lysates to Western blotting using streptavidin labeled with an infrared dye. Successful expression was verified by comparing the Western blot signals of the ORFs with a control protein lysate stock containing a PP-fusion of p21-activated kinase-2 (PAK2; Fig. 1). In earlier experiments we had confirmed that a reproducible selection of the same set of SH3 domains could be achieved over a wide range of PP-PAK2 expression levels (data not shown). A PP-PAK2-containg control lysate stock was used as a concentration standard to confirm an acceptable ORF expression by the individual PP-fusion clones, which was defined as a streptavidin blotting signal that was stronger than the signal observed for the lowest PP-PAK2 concentration that could still support robust and specific SH3 phage selection.

Of the 324 successfully expressed proteins 19 (5.6%) showed strong and selective SH3 binding, which was defined as >20-fold enrichment of infectious phages compared with
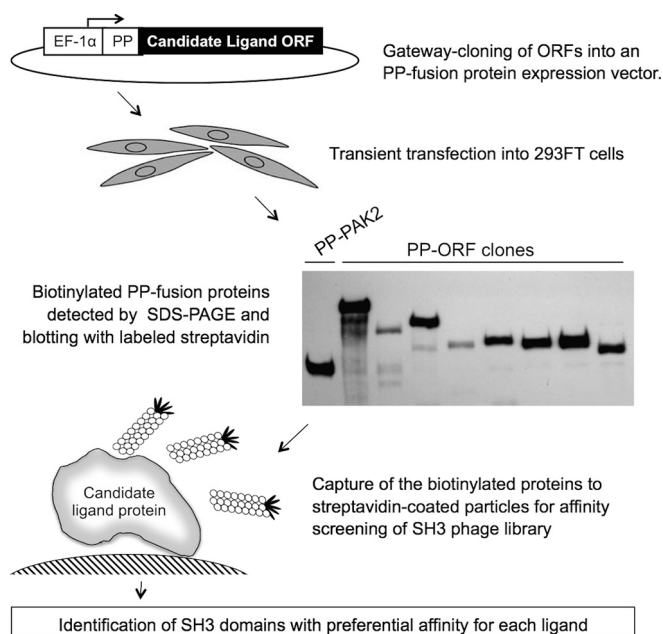
Fig. 1. **Schematic outline of the experimental strategy used.** Biotinylation domain (PP)-tagged putative ligand proteins were expressed by transient transfection, and immobilized onto streptavidin-coated paramagnetic beads. Subsequently a comprehensive library of human SH3 domain-expressing phages (296 different ones) was incubated with the potential ligand, followed by washing off the unbound phages, and infection of bacteria with the captured phages, and identification of these SH3 clones by DNA sequencing.

TABLE I

*Statistics of ORF expression and library screening results*

| | |
|---|---|
| Total number of ORFs selected for the study | 449 |
| ORFs successfully expressed and tested | 324 |
| • Strong and selective SH3 binders | 19 |
| • Significant binding but modest selectivity | 25 |
| • Poor or no binding | 298 |

mock panning (using control beads coated with an empty PP-domain only), and dominant selection of a just single or only a small number of individual SH3 domains. Significant enrichment of phages (between three- to 20-fold) samples associated with a lower SH3 binding selectivity was observed for another group of 25 proteins (7.7%). No significant SH3 binding and/or lack of specificity was observed for the remaining proteins, thus representing the majority (86%) of all the ORFs examined.

The 19 strong and selective SH3 ligands that we identified are listed in Table II together with their preferred SH3 partners revealed by the screen. Considering the unbiased selection strategy of the putative SH3 target proteins included in the screen, it was encouraging to find that these 19 best hits included some already described SH3-mediated proteins interactions that are known to involve distinctly high binding affinity and selectivity, namely the complex between GRB2-related adaptor protein downstream of Shc (GADS aka Mona)

and Src homology 2 domain-containing leukocyte phosphoprotein of 76 kDa (SLP-76 aka LCP2) (37, 38) and Hematopoietic cell-specific Lyn substrate 1 (HCLS1) interaction with the SH3 domain of Lyn (39).

However, the majority of the interactions that we discovered were novel. As evident from Table II, the robust enrichment of SH3 clones from the phage library was in most cases also associated with distinct selectivity. For example, the phage clones selected by HCLS1, Insulin receptor tyrosine kinase substrate (IRTKS), and Calcium/calmodulin-dependent protein kinase type IV (CAMK4) all involved only a single SH3 domain specific to these ligand proteins (Lyn, Eps8L3, and Btk, respectively). The single most preferred SH3 domain comprised 50% or more of the selected clones in 17 (out of 19) cases, and in the two remaining cases, namely Arg/Abl-interacting protein (ArgBP2) and Embryonal Fyn-associated substrate (EFS), half or more of the clones represented only two different SH3 domains. Of note, in several cases independent infectious preparations of the SH3 phage library were screened using independently prepared ligand proteins, confirming an excellent reproducibility of this. The data from such sub-screens for seven of the 19 ligand proteins listed in Table II are provided in supplemental Table S2.

*Functional Characterization of the Target Peptides in the SH3 Ligand Proteins*—To investigate the role of individual proline-rich motifs in SH3 binding by the 19 highly selective ligand proteins we synthetized 65 different peptides derived from these proteins (Table III). These peptide sequences were 15 to 17 residues in length, and overlapped with the predicted motifs that originally served as the criteria for selecting the corresponding proteins from the ORFeome v3.1 library. The number of potential target peptides contained in each ligand protein varied greatly, ranging from 1 (*e.g.* AMPH) to 12 (WIPF1).

These 65 peptides were spotted on glass slides and probed with 16 different SH3 domains, fused to the glutathione transferase (GST), including most of the SH3 domain that were highly selected from the phage library by at least one of target proteins. Some phage display-selected SH3 domains (GADS, Eps8L3, and Btk) could not be used because they were poorly expressed as recombinant proteins or showed nonspecific binding to the slides. To compensate for the lack of Eps8L3, the homologous SH3 domain of Eps8L1 was included as probe in these experiments. The most suitable concentration of the GST-SH3 proteins for probing of these arrays was empirically established as being 1 $\mu$M, which ensured the optimal peptide binding signal ratio over the background noise. Two different spatial spotting schemes were printed on each slide in order to exclude any position-related bias from the array signals, and three sets of 2 × 65 spotted peptides were probed with each SH3 domain. Representative sets of raw data from probing of these arrays with three different SH3 domains are shown in Fig. 2.

TABLE II
*Strong and selective SH3-binding ORFs and their SH3 partner preference*

| Ligand | Gene name(s) | Target SH3 | Share (%) |
|---|---|---|---|
| Hematopoietic cell-specific Lyn substrate | HCLS1, HS1 | Lyn | 100 |
| Insulin receptor tyrosine kinase substrate | IRTKS, BAIAP2L1 | Eps8L3 | 100 |
| Calcium/calmodulin-dependent protein kinase type IV | CAMK4 | Btk | 100 |
| SH2 domain containing leukocyte protein of 76kDa | SLP76, LCP2 | GADS (2/2) | 90 |
| | | Intersectin-1 (3/5) | 10 |
| c-Cbl-interacting protein of 85 kDa | CIN85, SH3KBP1 | Amphiphysin | 60 |
| | | SH3YL1 | 20 |
| | | Crk (1/2) | 13 |
| | | CrkL (1/2) | 7 |
| SH2-B homolog | SH2B, PSM | Lyn | 64 |
| | | SH3YL1 | 36 |
| Neutrophil cytosolic factor 2 | NCF2, p67phox | Ponsin (2/3) | 75 |
| | | ArgBP2 (2/3) | 13 |
| | | IRTKS | 6 |
| | | Tec | 6 |
| Neutrophil cytosolic factor 1 | NCF1, p47phox | AHI-1 | 42 |
| | | OSTF1 | 23 |
| | | Ponsin (2/3) | 15 |
| | | SH3YL1 | 8 |
| | | POSH (4/4) | 4 |
| | | Tec | 4 |
| | | NBL1 | 4 |
| Arg/Abl-interacting protein | ArgBP2, SORBS2 | CMS (1/3) | 35 |
| | | Tec | 25 |
| | | AHI-1 | 15 |
| | | Src | 15 |
| | | Lyn | 10 |
| Amphiphysin1 | AMPH | ArgBP2 (2/3) | 58 |
| | | Ponsin (2/3) | 42 |
| Testis-specific kinase 1 | TESK1 | ARHGEF37 (2/2) | 63 |
| | | Src | 13 |
| | | OSTF1 | 13 |
| | | FISH (3/5) | 13 |
| SH3 domain containing, Ysc84-like 1 | SH3YL1 | Src | 69 |
| | | CMS (1/3) | 31 |
| PDZ domain containing 8 | PDZK8 | Intersectin-1 (3/5) | 88 |
| | | Intersectin-2 (3/5) | 13 |
| Embryonal Fyn-associated substrate | EFS, SIN | Src | 25 |
| | | Yes | 25 |
| | | Btk | 25 |
| | | Nephrocystin | 13 |
| | | Tec | 13 |
| PHD finger protein 21B | PHF21 B | Src | 43 |
| | | Fyn | 43 |
| | | Nephrocystin | 14 |
| DENN domain-containing protein 1A | DENND1A | CrkL (1/2) | 71 |
| | | Amphiphysin | 29 |
| Signal transduction protein CBL-C | CBLC, CBL-3 | Tec | 75 |
| | | SH3YL1 | 13 |
| | | Intersectin-1 (3/5) | 13 |
| WAS/WASL interacting protein family, member 1 | WIPF1, WASPIP | Src | 63 |
| | | Btk | 13 |
| | | Lyn | 13 |
| | | Tec | 13 |
| ArfGAP with SH3 domain, ankyrin repeat and PH domain 2 | ASAP2, AMAP2, DDEF2, PAG3 | Src | 71 |
| | | Btk | 14 |
| | | Intersectin-1 (3/5) | 14 |

TABLE III

*Summary of the peptide array data. The sequences of the arrayed peptides covering the potential target motifs in the 19 ligand proteins are shown, and the relative intensity of their binding to the 16 SH3 domains used as probes is indicated. The binding intensity values are highlighted according to the categories described in the text (strong = pink, intermediate = orange, weak = grey, negative = no color). The binding values for peptides derived from ligand proteins that specifically selected the corresponding SH3 domain from the phage library are boxed, indicating >5% (black square) or >50% (blue square) proportion of all the SH3 domains selected by this ligand protein. The IRTKS peptide is circled in blue for EpsL1-SH3, although the highly selected SH3 domain for IRTKS was the closely related Eps8L3, which was not available as a probe. Other highly selected SH3 domains that could not be produced as a high quality probes were Btk, ponsin (2/3), GADS (2/2), and ARHGEF37*

| Ligand | Peptide No. | Sequence | Amph | ArgBP2(2/3) | CIN85 (1/3) | CMS (1/3) | CrkL (1/2) | Eps8L1 | Fyn | IRTKS | ITSN1 (3/5) | ITSN2 (3/5) | Lyn | NPHP1 | OSTF1 | Src | Tec | Yes |
|---|---|---|---|---|---|---|---|---|---|---|---|---|---|---|---|---|---|---|
| Amph | 21 | RSPSQTRKGPPVPPLPKV | 1,18 | 0,49 | 0,23 | 0,72 | 0,15 | 0,21 | 0,22 | 0,42 | 0,07 | 0,11 | 0,04 | 0,02 | 0,03 | 0,03 | 0,15 | 0,08 |
| ArgBP2 | 15 | PPPHVPPPVPPLRPRDRS | 1,38 | 2,45 | 3,25 | 3,79 | 1,10 | 0,48 | 3,80 | 0,52 | 2,00 | 1,95 | 1,91 | 0,42 | 2,43 | 2,19 | 2,17 | 2,51 |
|  | 16 | PPPLPTTPTPVPREPGRK | 0,51 | 0,32 | 2,11 | 5,09 | 0,20 | 0,28 | 0,09 | 0,39 | 0,21 | 0,20 | 0,18 | 0,25 | 0,15 | 0,11 | 0,09 | 0,17 |
|  | 17 | EVTGSPSPPPRSGAPTPS | 1,03 | 0,31 | 5,13 | 3,94 | 2,09 | 0,20 | 0,21 | 0,63 | 2,44 | 1,54 | 1,71 | 1,25 | 3,54 | 1,54 | 1,87 | 0,37 |
|  | 18 | SRAPALSPTRPPKKPLDY | 1,29 | 0,46 | 0,23 | 0,10 | 0,13 | 0,61 | 0,41 | 0,63 | 0,19 | 0,10 | 0,13 | 0,06 | 0,09 | 0,06 | 0,35 | 0,19 |
|  | 19 | KSFTSSSPSSPSRAKDRE | 1,34 | 0,34 | 0,27 | 0,09 | 0,11 | 0,42 | 0,48 | 1,06 | 0,20 | 0,17 | 0,17 | 0,08 | 0,07 | 0,06 | 0,08 | 0,22 |
|  | 20 | KLTPPEKAQPARPPPPAQ | 1,97 | 3,20 | 0,11 | 0,13 | 1,95 | 0,60 | 0,21 | 0,66 | 0,11 | 0,53 | 0,26 | 0,98 | 0,16 | 0,29 | 0,19 | 0,10 |
| ASAP2 | 60 | QPAAPSTTSAPPLPPRNV | 1,26 | 0,99 | 8,90 | 4,68 | 7,58 | 2,78 | 5,53 | 1,17 | 4,63 | 3,77 | 3,62 | 3,15 | 4,75 | 3,77 | 4,75 | 8,03 |
|  | 61 | ISQIRPPPLPPQPPSRLP | 1,81 | 3,91 | 6,60 | 3,14 | 3,66 | 2,29 | 3,80 | 5,42 | 2,23 | 2,64 | 3,23 | 2,56 | 3,12 | 3,51 | 3,15 | 3,31 |
|  | 62 | KPAPPGISQIRPPPLPPQ | 1,62 | 0,98 | 1,03 | 0,49 | 1,04 | 1,20 | 1,17 | 1,63 | 1,77 | 1,79 | 1,31 | 2,96 | 2,16 | 2,35 | 3,39 | 1,32 |
|  | 63 | LPPQPPSRLPQKKPAPGA | 1,78 | 0,93 | 0,29 | 0,30 | 1,84 | 1,49 | 1,05 | 0,79 | 0,18 | 0,18 | 0,40 | 0,07 | 0,15 | 0,17 | 0,11 | 0,15 |
|  | 64 | DKSTPLTNKGQPRGPVDL | 1,25 | 0,21 | 0,11 | 0,20 | 0,07 | 0,44 | 0,20 | 0,71 | 0,09 | 0,15 | 0,07 | 0,13 | 0,03 | 0,06 | 0,06 | 0,10 |
|  | 65 | NAMVLQPPAPMPRKSQAT | 1,53 | 0,31 | 0,91 | 3,40 | 0,05 | 0,54 | 0,27 | 0,77 | 0,11 | 0,25 | 0,10 | 0,17 | 0,05 | 0,02 | 0,04 | 0,10 |
| CAMK4 | 43 | NLLYATPAPDAPLKIADF | 0,37 | 0,19 | 0,04 | 0,02 | 0,06 | 0,56 | 0,11 | 0,20 | 0,05 | 0,11 | 0,03 | 0,07 | 0,02 | 0,02 | 0,02 | 0,32 |
| CBLC | 47 | LSAPPLPPRPDLPPRKPR | 1,73 | 5,04 | 3,50 | 2,96 | 9,26 | 5,73 | 4,70 | 3,46 | 4,72 | 4,60 | 4,85 | 3,61 | 4,80 | 5,21 | 5,21 | 4,56 |
| CIN85 | 6 | KHEIKKIPPERPEMLPNR | 0,99 | 0,44 | 0,31 | 0,19 | 0,36 | 0,70 | 0,23 | 0,55 | 0,15 | 0,25 | 0,10 | 0,15 | 0,09 | 0,06 | 0,08 | 0,09 |
|  | 7 | QKPSVPAIPPKKPRPPKT | 0,95 | 0,71 | 0,15 | 2,43 | 7,35 | 1,20 | 0,19 | 0,50 | 0,19 | 0,36 | 0,16 | 0,07 | 0,06 | 0,03 | 0,08 | 0,14 |
|  | 8 | RPGALPPRRPERPVGPLT | 1,54 | 1,80 | 0,54 | 1,29 | 0,50 | 0,32 | 0,35 | 0,42 | 1,00 | 1,13 | 0,42 | 0,92 | 0,16 | 0,17 | 0,41 | 0,07 |
| DENND1A | 45 | TVPDTRELPSIPENRNLT | 0,29 | 0,18 | 0,08 | 0,04 | 0,08 | 0,28 | 0,25 | 0,26 | 2,34 | 2,22 | 1,94 | 3,18 | 1,25 | 2,11 | 0,93 | 1,70 |
|  | 46 | RNALKIEPEEPITFCEEA | 0,91 | 0,73 | 0,15 | 0,18 | 0,42 | 1,05 | 0,49 | 0,52 | 0,35 | 0,34 | 0,26 | 0,23 | 0,36 | 0,25 | 0,30 | 0,32 |
| EFS | 38 | HPLTRVAPQPPGEDDAPY | 0,71 | 2,14 | 0,06 | 0,03 | 0,12 | 1,16 | 0,34 | 0,39 | 0,21 | 0,36 | 0,51 | 0,91 | 0,11 | 0,04 | 0,14 | 0,14 |
|  | 39 | QLLARSPPPPHRPRLPSA | 1,20 | 1,62 | 0,25 | 0,28 | 0,30 | 1,34 | 1,36 | 1,14 | 0,53 | 0,72 | 1,37 | 0,74 | 0,43 | 0,42 | 0,37 | 0,55 |
|  | 40 | ESLSRRPLPALPVPEAPS | 0,69 | 1,00 | 1,49 | 1,03 | 2,98 | 3,52 | 6,46 | 0,90 | 3,97 | 4,15 | 3,57 | 4,29 | 4,38 | 5,18 | 4,84 | 8,23 |
|  | 41 | KGSIQDRPLPPPPPRLPG | 1,01 | 2,84 | 4,36 | 2,08 | 2,56 | 1,80 | 5,58 | 6,90 | 3,18 | 3,06 | 2,86 | 2,84 | 3,99 | 3,49 | 3,37 | 5,25 |
|  | 42 | QACTGDPELPERGMPAPQ | 0,35 | 0,22 | 0,11 | 0,02 | 0,06 | 0,27 | 0,24 | 0,23 | 0,05 | 0,15 | 0,08 | 1,21 | 0,05 | 0,12 | 0,05 | 0,16 |
| HCLS1 | 1 | TSREHPVPLLPIRQTLPE | 0,36 | 0,31 | 0,13 | 0,13 | 0,68 | 0,60 | 0,06 | 0,96 | 0,70 | 0,85 | 1,10 | 1,67 | 0,25 | 0,79 | 0,26 | 0,05 |
|  | 2 | EDNEEPPALPPRTLEGLQ | 0,44 | 0,69 | 0,08 | 0,27 | 1,52 | 0,22 | 0,15 | 0,26 | 1,40 | 0,84 | 2,11 | 1,76 | 0,83 | 1,38 | 1,96 | 0,08 |
|  | 3 | PEPEPEPEPEPENDYEDV | 1,24 | 0,91 | 0,16 | 0,09 | 0,07 | 0,98 | 0,44 | 0,28 | 0,20 | 0,15 | 0,10 | 0,09 | 0,09 | 0,06 | 0,13 | 0,17 |
|  | 4 | DRHEQEDEPEGDYEEVLE | 1,44 | 0,85 | 0,11 | 0,07 | 0,15 | 1,20 | 0,53 | 0,47 | 0,25 | 0,19 | 0,05 | 0,09 | 0,09 | 0,05 | 0,12 | 0,19 |
| IRTKS | 5 | ENSSVVIPPPDYLECLSM | 0,48 | 0,31 | 0,09 | 0,04 | 0,06 | 10,87 | 0,13 | 0,26 | 0,10 | 0,17 | 0,04 | 0,12 | 0,07 | 0,05 | 0,06 | 0,04 |
| NCF1 | 12 | NPENRIIPHLPAPKWFDG | 0,25 | 0,21 | 0,04 | 0,03 | 0,04 | 0,35 | 0,11 | 0,47 | 0,09 | 0,12 | 0,07 | 0,24 | 0,05 | 0,09 | 0,08 | 0,04 |
|  | 13 | RRQARPGPQSPGSPLEEE | 1,04 | 0,94 | 0,11 | 0,10 | 0,03 | 1,69 | 0,24 | 0,28 | 0,22 | 0,24 | 0,11 | 0,15 | 0,18 | 0,05 | 0,14 | 0,13 |
|  | 14 | QTQRSKPQPAVPPRPSAD | 1,84 | 3,72 | 3,71 | 2,91 | 0,37 | 0,49 | 0,51 | 0,58 | 2,96 | 2,55 | 2,49 | 1,52 | 3,31 | 2,19 | 2,43 | 0,52 |
| NCF2 | 11 | KYTVVMKTQPGLPYSQVR | 0,95 | 0,26 | 0,50 | 0,21 | 0,19 | 0,33 | 0,14 | 0,66 | 0,13 | 0,12 | 0,09 | 0,07 | 0,04 | 0,03 | 0,05 | 0,18 |
| PDZK8 | 30 | LAQFFLLYRRQPEPPADE | 0,35 | 0,66 | 0,23 | 0,21 | 0,08 | 0,74 | 0,14 | 0,34 | 0,16 | 0,22 | 0,12 | 0,16 | 0,12 | 0,10 | 0,14 | 0,25 |
|  | 31 | AAPETPAPPTRETCYFLN | 0,21 | 0,19 | 0,22 | 0,22 | 0,11 | 0,21 | 0,06 | 0,28 | 0,11 | 0,12 | 0,10 | 0,06 | 0,07 | 0,04 | 0,05 | 0,14 |
|  | 32 | NYKIRFKPFFPYQTLQGF | 0,28 | 0,55 | 2,27 | 0,49 | 0,37 | 0,39 | 0,16 | 1,66 | 0,42 | 0,35 | 0,28 | 0,22 | 0,44 | 0,22 | 0,37 | 0,59 |
|  | 33 | QGSAFKPPVPPRPQAKVP | 2,44 | 4,18 | 3,57 | 3,31 | 2,88 | 0,77 | 2,32 | 0,63 | 3,28 | 3,83 | 2,94 | 1,08 | 3,49 | 3,47 | 3,52 | 1,10 |
|  | 34 | DTEVCGPNSPSKRGNSTG | 0,50 | 0,31 | 0,16 | 0,07 | 0,30 | 0,26 | 0,13 | 0,47 | 0,20 | 0,20 | 0,19 | 0,11 | 0,11 | 0,08 | 0,13 | 0,19 |
| PHF21B | 44 | DSLPVAPGRDRPPKQPPT | 0,12 | 0,29 | 0,22 | 4,90 | 0,11 | 0,16 | 0,22 | 0,87 | 0,66 | 0,34 | 0,21 | 0,42 | 0,16 | 0,13 | 0,19 | 0,22 |
| SH2B1 | 9 | ECLSPGPCPATSPRPMTL | 0,33 | 0,19 | 0,29 | 0,22 | 0,12 | 0,21 | 0,09 | 0,28 | 0,19 | 0,30 | 0,17 | 0,10 | 0,07 | 0,06 | 0,13 | 0,06 |
|  | 10 | DSMELLPPELPPRIPIEE | 0,69 | 1,05 | 0,11 | 0,09 | 0,19 | 1,21 | 0,24 | 0,26 | 1,81 | 1,11 | 2,43 | 1,25 | 0,58 | 1,00 | 1,58 | 0,10 |
| SH3YL1 | 29 | REQRKSSAKELPPKPLSR | 1,00 | 0,54 | 0,27 | 0,91 | 0,14 | 0,50 | 0,36 | 0,63 | 0,19 | 0,20 | 0,17 | 0,17 | 0,13 | 0,15 | 0,14 | 0,18 |
| SLP76 | 35 | QQPPVPPQRPMAALPPPP | 0,37 | 1,36 | 2,80 | 2,06 | 0,18 | 0,22 | 0,23 | 1,84 | 2,07 | 1,75 | 1,17 | 1,72 | 1,79 | 1,40 | 2,83 | 1,29 |
|  | 36 | RSTKPSPMNLPLPSSHMPG | 1,45 | 0,46 | 0,11 | 0,05 | 0,11 | 0,72 | 0,36 | 0,50 | 0,12 | 0,13 | 0,08 | 0,18 | 0,07 | 0,07 | 0,06 | 0,10 |
|  | 37 | NFPLPLPNKPRPPSPAEE | 0,53 | 2,04 | 0,15 | 0,28 | 1,85 | 1,28 | 0,31 | 0,61 | 0,68 | 0,90 | 0,80 | 1,42 | 0,64 | 1,06 | 0,61 | 0,39 |
| TESK1 | 22 | RVPADPDYLPRTEDFGLD | 0,99 | 0,46 | 0,11 | 0,07 | 0,40 | 0,71 | 0,29 | 0,42 | 0,16 | 0,16 | 0,09 | 0,06 | 0,05 | 0,05 | 0,06 | 0,16 |
|  | 23 | GPSATLPRPDPRLSRSRS | 0,98 | 0,37 | 0,15 | 0,14 | 0,14 | 0,32 | 0,34 | 0,98 | 0,20 | 0,19 | 0,16 | 0,09 | 0,05 | 0,04 | 0,06 | 0,19 |
|  | 24 | LVTTPETLVQPGTPARRC | 0,53 | 0,17 | 0,06 | 0,07 | 0,40 | 0,25 | 0,15 | 0,44 | 0,15 | 0,19 | 0,12 | 0,15 | 0,07 | 0,05 | 0,07 | 0,15 |
|  | 25 | RRCRSLPSSPELPRRMET | 0,58 | 0,24 | 0,15 | 0,18 | 0,86 | 0,32 | 0,25 | 0,28 | 1,22 | 1,06 | 1,07 | 1,96 | 0,22 | 0,76 | 0,32 | 0,42 |
|  | 26 | TLVQPGTPARRCRSLPSS | 0,56 | 0,25 | 0,16 | 0,25 | 0,15 | 0,46 | 0,30 | 0,58 | 0,16 | 0,19 | 0,15 | 0,84 | 0,08 | 0,06 | 0,07 | 0,18 |
|  | 27 | LPSSPELPRRMETALPGP | 0,34 | 0,19 | 0,04 | 0,02 | 0,13 | 0,22 | 0,13 | 1,52 | 0,19 | 0,28 | 0,18 | 0,26 | 0,04 | 0,10 | 0,11 | 0,09 |
|  | 28 | ALERTEPSPPPSAPREPD | 0,25 | 0,20 | 0,06 | 0,02 | 0,05 | 0,31 | 0,13 | 0,31 | 0,04 | 0,10 | 0,04 | 0,66 | 0,02 | 0,02 | 0,02 | 0,06 |
| WIPF1 | 48 | KPFSPPSGPGRFPVPSPG | 1,02 | 0,57 | 0,73 | 0,23 | 0,20 | 1,17 | 0,40 | 0,69 | 0,27 | 0,36 | 0,33 | 0,23 | 0,25 | 0,36 | 1,10 | 0,44 |
|  | 49 | FPVPSPGHRSGPPEPQRN | 0,99 | 0,43 | 0,27 | 0,77 | 0,14 | 0,92 | 0,71 | 0,36 | 0,83 | 1,19 | 0,44 | 1,73 | 0,20 | 1,70 | 0,89 | 1,54 |
|  | 50 | QRNRMPPPRPDVGSKPDS | 1,86 | 0,82 | 1,42 | 1,58 | 0,13 | 1,06 | 0,60 | 0,69 | 1,13 | 1,54 | 1,11 | 2,42 | 0,48 | 0,18 | 0,82 | 0,39 |
|  | 51 | QSSLHNRGSPPVPGGPRQ | 1,41 | 0,40 | 0,11 | 0,05 | 0,07 | 0,48 | 0,56 | 0,36 | 0,10 | 0,17 | 0,45 | 0,35 | 0,07 | 0,13 | 0,11 | 0,11 |
|  | 52 | QPSPGPTPPPPPVRDPPG | 0,42 | 1,30 | 0,96 | 1,64 | 0,79 | 0,42 | 0,30 | 2,89 | 1,59 | 2,04 | 1,81 | 0,62 | 2,88 | 2,11 | 1,36 | 2,04 |
|  | 53 | DPPGRSGPLPPPPPVSRN | 1,77 | 2,34 | 1,62 | 2,19 | 1,22 | 0,48 | 4,72 | 1,63 | 2,23 | 2,05 | 2,99 | 2,32 | 3,19 | 3,28 | 2,82 | 4,96 |
|  | 54 | NGSTSRALPATPQLPSRS | 2,22 | 0,41 | 0,96 | 1,72 | 5,14 | 0,95 | 3,78 | 0,87 | 4,39 | 3,48 | 3,35 | 3,43 | 4,06 | 4,09 | 3,22 | 4,66 |
|  | 55 | PPPVSRNGSTSRALPATP | 1,17 | 0,32 | 0,23 | 0,07 | 0,22 | 0,69 | 1,41 | 0,42 | 2,46 | 2,58 | 2,34 | 2,65 | 1,63 | 2,43 | 1,63 | 2,35 |
|  | 56 | ATPQLPSRSGVDSPRSGP | 0,88 | 0,42 | 0,68 | 0,09 | 0,18 | 0,51 | 0,74 | 0,61 | 0,22 | 0,33 | 0,23 | 0,38 | 0,22 | 0,18 | 0,21 | 0,23 |
|  | 57 | DSPRSGPRPPLPPDRPSA | 2,09 | 2,07 | 1,21 | 1,43 | 0,28 | 1,50 | 2,63 | 1,12 | 2,04 | 2,05 | 2,48 | 1,00 | 3,22 | 2,41 | 2,26 | 1,34 |
|  | 58 | PLPPDRPSAGAPPPPPPS | 0,27 | 0,28 | 0,08 | 0,06 | 0,06 | 0,49 | 0,14 | 7,01 | 0,28 | 0,62 | 0,60 | 0,61 | 1,70 | 1,09 | 1,38 | 0,22 |
|  | 59 | SGSNRRERGAPPLPPIPR | 1,63 | 1,91 | 0,48 | 0,96 | 0,56 | 0,83 | 2,77 | 0,77 | 0,45 | 0,94 | 2,95 | 2,29 | 1,59 | 1,61 | 1,31 | 1,30 |

Src SH3

ITSN1 (3/5) SH3

Eps8L1 SH3

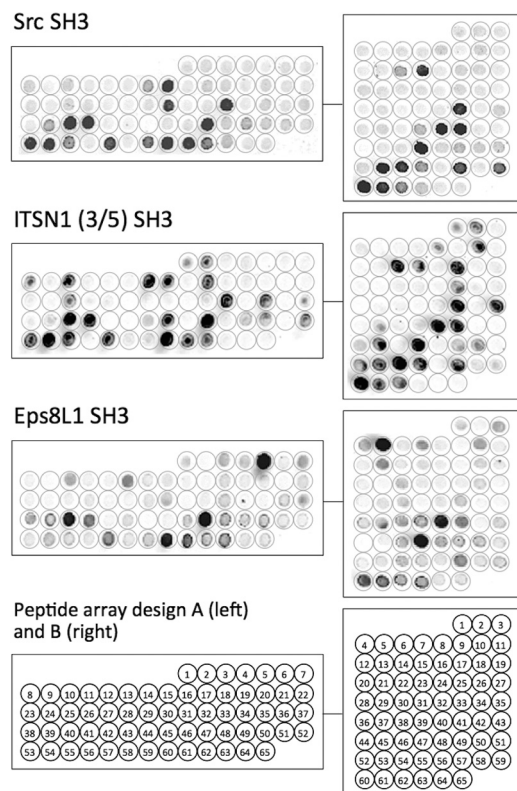Peptide array design A (left) and B (right)

FIG. 2. **Raw data from probing of the peptide arrays with three different SH3 domains.** The 65 peptides were spotted using two different schemes and probed with the indicated GST-tagged SH3 domains, followed by detection of binding with a labeled anti-GST antibody.

Because of the nature of this experimental approach, a direct comparison of the absolute binding signals obtained from probing of the peptide array slides with different GST-SH3 probes would not be informative. Instead, we compared the relative peptide binding signals measured for each SH3 domain. After subtracting background fluorescence values from the peptide spot signals, the SH3 binding intensity value of each peptide was calculated relative to the average signal of all the peptides in the same array (see Table III).

For discussion purposes we divided the relative SH3 binding by these peptides into four categories; negative, weak, intermediate, and strong. Signals that were below the half of the average (<0.5) of all the peptides were scored as "negative." Signals that were 0.50–0.99 times the average were scored as "weak," 1.0–1.99 times the average as "intermediate," and twice the average or higher (>2) as "strong." Depending on the SH3 domain used as a probe 4.6–23.1% (3–15 out of 65) of the peptides scored as strong binders, 6.2–43.1% (4–28) as intermediate binders, 4.6–36.9% (3–24) as weak binders, and 26.2–69.2% (17–45) as "negative." These differences reflected the variable peptide binding selectivity of the different SH3 domains tested, but to some extent also the experimental signal to noise ratio determined by the technical quality of the individual GST-SH3 probes. In

the case of a highly selective binder, such as Eps8L1 SH3, the strongest signal was more than 10 times the average, whereas this ratio was less than 3 for some SH3 domains, such as amphiphysin.

The 65 putative target peptides varied greatly in their relative specificity as SH3 targets. Some peptides were highly promiscuous in SH3 binding. Ten of these peptides were good binders (strong or intermediate) for more than 80% of the SH3 domains (at least 13 of the 16 SH3 probes), including three peptides (ISQIRPPPLPPQPPSRLP, LSAPPLPPRPDLP-PRKPR and KGSIQDRPLPPPPPRLPG from ASAP2, CBLC, and EFS respectively), which scored as strong binders for all SH3 domains except amphiphysin. On the other hand, many peptides showed distinct SH3 selectivity. More than a third of the peptides ($n = 24$; 37%) were strong or intermediate binders for only three or fewer of the 16 SH3 probes, including six peptides with strong binding to one or two SH3 domains, but weak or negative binding to the remaining 14 SH3 domains. The highest specificity was presented by the peptide ENSS-VVIPPPDYLECLSM from IRTKS that bound very intensely (more than 10 times average) to Eps8L1, but scored negative for all other SH3 domains. Although this specificity agrees well with the known preference of the Eps8-family SH3 domains for PxxDY motif-containing ligands (9), it is interesting to note that within this family Eps8L3 SH3 appears to be the superior binder for native IRTKS protein, as it was able to outcompete other SH3 domains in the library (including Eps8L1) and alone dominate the screening results. Other examples of peptides showing strong and selective binding were the ArgBP2 SH3#2 binder HPLTRVAPQPPGEDDAPY (from Efs), the CMS SH3 (1/3) binder DSLPVAPGRDRP-PKQPPT (from PHF21B), the CIN85 SH3 (1/3) binder NYKIR-FKPFFPYQTLQGF (from PDZK8), and the CrkL and CMS SH3 (1/3) binder QKPSVPAIPPKKPRPPKT (from CIN85). Fourteen peptides (22%) did not show higher than average binding to any SH3 probe, but of note, only three (4.6%) scored negative for all SH3 domains.

As might be expected, the phage library screening and the peptide array binding data sets showed some correlation with each other. At least one peptide with stronger than average binding to an SH3 domain was more often present than lacking in ligand proteins that had affinity-selected the same SH3 domain from the phage library. However, considering that almost half of the ligand proteins contained one or more peptides showing strong and highly promiscuous SH3 binding this overlap is not very striking. Indeed, if the six most promiscuous peptides in the array (from ASAP2, Efs, CBLC, PDZK8) that dominated the top scoring SH3 target peptide lists were excluded, only two peptides derived from their preferred native ligand proteins could be found among the strongest 10% binding peptides for the same SH3 domains. These were ENSSVVIPPPDYLECLSM from IRTKS and QKPSVPAIPPKKPRPPKT from CIN85, which were the best

and the third best binding peptides of Eps8L1 SH3 and CrkL SH3 (1/2), respectively.

On the other hand, several ligand proteins that showed strong selection of individual SH3 domains from the phage library did not contain a peptide capable of higher than average binding to these SH3 domains. A striking example of this was PHF21B that preferentially selected Fyn and Src SH3 domains as its partners from the phage library. PHF21B contains a single proline-rich motif (DSLPVAPGRDRPPKQPPT) that in the peptide array showed strong (almost five times the average) and highly selective binding to CMS SH3 (1/3), but was negative for Fyn and Src.

In summary, based on the divergent and reproducible binding patterns obtained with different SH3 probes, together with the low proportion of peptides failing to show any SH3 binding we conclude that the technical quality of these peptide array data was good. Nevertheless, the binding strength of individual SH3 interaction motifs failed to predict preferred partnerships revealed by these ligand proteins in their native form.

*Semiquantitative Analysis of the Strength of Selected SH3-ligand Protein Interactions*—Because the strong and preferred SH3 interactions identified by phage library screening correlated poorly with SH3 binding selectivity of short linear peptides derived from the same target proteins it was of interest to study binding of these ligand proteins to SH3 domains in solution. Such studies were also necessary to substantiate our premise that robust and dominant interactions revealed by screening of the SH3 proteome phage library involve significantly higher binding affinities than those reported for most SH3 interactions.

To address these issues we established a semiquantitative pull-down assay where paramagnetic streptavidin beads coated with biotin-tagged ligand proteins derived from human 293T cells were incubated with known concentrations of recombinant SH3 domains. In preparatory experiments (not shown) we first tested and validated this assay system the amounts of SH3 captured by HIV-1 Nef-coated beads incubated with serial dilutions of Hck SH3 were examined by Scatchard analysis, which gave a $K_D$ value of 189 nM matching relatively closely the value of 250 nM previously established for this high-affinity SH3 interaction in proper quantitative measurements (10, 11). Thus, despite the limitations of this semiquantitative system, involving beads densely coated with the ligand and a non-equilibrium incubation phase (*i.e.* including washes) it was found to be adequate for estimating of binding affinities, at least for strong (submicromolar range) SH3 interactions.

Four ligand proteins (SH3YL1, SH2B, DENND1A, and PHF21B) that in phage library screening showed different binding preferences toward the SH3 domains of Src, Lyn, CrkL, and Fyn (Fig. 3*A*) were chosen for comparison. Similar to the library screening (see Fig. 1) these ligands were expressed as native, biotinylation domain-tagged proteins in human cells, and immobilized on paramagnetic beads. When beads coated with SH3YL1 were incubated with soluble Src, Lyn, CrkL, and Fyn SH3 domains at a 500 nM concentration, washed, and examined for the associated SH3 domains, a highly preferential binding to Src-SH3 was observed, whereas only weak binding to the three other SH3 domains was observed, (Fig. 3*B*).

This agreed well with the preferential (69%) selection of Src SH3-displaying phage clones in the library screen, and is striking also when considering that Lyn and Fyn belong to the same Src-family of SH3 domains, and are known to prefer similar core SH3 binding motifs (40). Likewise, a clearly preferential pull-down of Lyn-SH3 was observed for SH2B (Fig. 3*C*), which in the SH3 phage screening showed exclusive selection (100%) of Lyn as its binding partner. DENND1A that showed 71% selection of CrkL SH3 in phage screening also preferentially associated with CrkL in this pull-down comparison, although its selectivity at the 500 nM SH3 concentration tested was less striking than observed for SH3YL1 and SH2B. However, considering that DENND1A does not contain a peptide showing even intermediate level binding to CrkL SH3, this agreement with the preference of native DENND1A for CrkL observed in phage screening is remarkable. Finally, PHF21B that preferred Src as well as Fyn SH3 domain (both 43% of selected clones) in library screens, also bound to these two SH3 domains more strongly than to Lyn or CrkL. In conclusion, the results obtained in this pull-down assay including four SH3 ligand proteins *versus* four selected SH3 domains correlated well with the binding preferences identified for these native ligands, but agreed poorly with the peptide array data, and in some cases (for example PHF21B) even contrasted the SH3 binding profiles of isolated proline-rich peptides from the same proteins.

To estimate the binding affinity involved in the dominant SH3 - ligand partnerships revealed by the SH3 library screens we chose two such interactions for more detailed analyses. One was binding of HCLS1 to Lyn-SH3, which similar to the SH2B/Lyn interaction was suggested to be of high affinity by the exclusive affinity selection of Lyn-SH3 by HCLS1 from the phage library. The other one was the SH3YL1/Src-SH3 interaction, which appeared to be particularly strong when examined for its selectivity in Fig. 3*B*. Dilution series of Lyn and Src SH3 domains were incubated with beads coated with their cognate ligand proteins, and their association with HCLS1 and SH3YL1 was examined with the pull-down assay described above (Figs. 3*F* and 3*G*). When the capacity of HCLS1 and SH3YL1 to capture Lyn and Src SH3 domains provided at different concentrations was quantified and examined by Scatchard analysis (Fig. 3*H*), submicromolar affinity values indicative of exceptionally tight SH3 binding could be determined. The $K_D$ value of the HCLS1/Lyn-SH3 interaction was estimated to be 746 nM, whereas an affinity as high as 187 nM was found for the SH3YL1/Src-SH3 complex. By contrast, when binding of HCLS1 to Fyn-SH3 was tested an affinity of only 7 $\mu$M was measured (supplemental Fig. S1).

FIG. 3. **Selectivity and affinity of binding of four selected ligand proteins to recombinant SH3 domains in solution.** *A,* The quality and concentration of purified Src, Lyn, Fyn. and CrkL SH3 domains expressed as biotinylated GST fusion proteins in *E. coli* were confirmed by running a calculated 50 ng of each in SDS-PAGE followed by Western blotting (*B* to *E*). The SH3 ligand proteins SH3YL1 (*A*), SH2B (*B*), DENND1A (*C*), and PHF21B (*D*) were expressed in human 293T cells by transient transfection, and immobilized on paramagnetic beads. These ligand-coated beads were added to a control tube (-) and to tubes containing a 500 nM solution of Src, Lyn, Fyn, or CrkL SH3. After incubation the beads were washed to remove unbound SH3, followed by analysis of the coated ligand proteins and the associated SH3 domains by SDS-PAGE and Western blotting. The intensities of the specific ligand-captured SH3 signals were quantified, and are shown above the corresponding blots as bar graphs where the strongest signal has been normalized to a value of 100 (*F* and *G*). Aliquots of beads coated with HCLS1 (*F*) or SH3YL1 (*G*) as described above were similarly incubated with increasing concentrations (from 0 to 4 $\mu$M) of Lyn-SH3 (*F*) or Src-SH3 (*G*), followed by analysis and quantification of ligand-bound SH3 domains as above. *H,* The signal intensities of the specifically captured SH3 domains were examined by Scatchard analysis to derive the indicated $K_D$ values for the HCLS1/Lyn-SH3 and the SH3YL1/Src-SH3 interactions. The $R^2$ values describing the goodness of fit for the data points in the Scatchard analysis were 0.9035 and 0.9256, respectively.
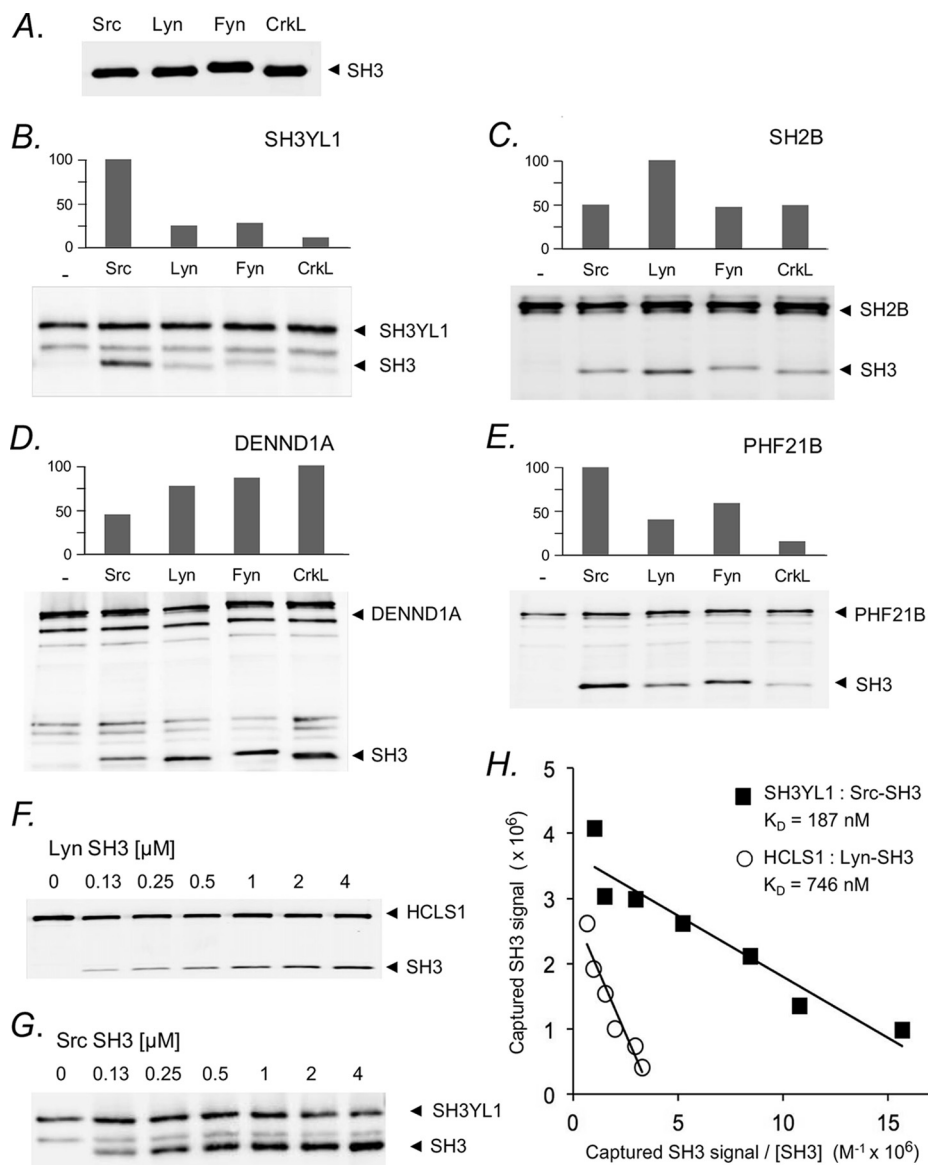


Together these semi-quantitative interaction data support the validity of our phage library results and the notion that these screens can provide novel examples of high affinity SH3 interactions where the binding strength and specificity cannot be recapitulated by short linear peptide ligands.

DISCUSSION

In this study we have made use of a phage display library that contains a near complete collection of human SH3 domains to carry out a large-scale protein interaction screen involving hundreds of potential human SH3 ligand proteins. A key objective of our study was to systematically examine how commonly strong and selective interactions occur among the human "SH3 interactome." In addition, identification of such robust SH3 interactions could provide valuable new leads for research aimed at unraveling signaling protein networks that regulate cell behavior.

The use of full-length ligand proteins in this study ensured that complex interactions involving binding determinant outside of the predicted SH3 target site would not be missed. To make sure that these full-length proteins are produced and folded properly, we produced them in mammalian (HEK293T) cells. Of the total 449 potential SH3 ligand proteins predicted from the human genome 324 could be produced successfully as judged by an expectedly sized Western blotting signal with an acceptable intensity.

The phage library that we used has previously proven its value in identifying high-affinity SH3 partners for a number of cellular and pathogen-encoded ligand proteins (12–25). These studies have established the positive predictive value of the hits generated by this screening method to be remarkably high, *i.e.* the preferred SH3-ligand partnerships revealed by the library screens have reliable indicated cellular interactions

that have subsequently been readily verified biochemically/ functionally. In part, this success can be explained by the inherent feature of this experimental system of failing to detect SH3 interactions with low/modest affinity. Although many weak but potentially relevant interactions may thus be missed, the false discovery rate remains low. For example, although the HIV Nef protein is well documented to interact with the Src-family kinase SH3 domains Lck and Fyn (affinities 10.6 $\mu M$ and 15.8 $\mu M$; (41)), only the high-affinity SH3 partners Hck (affinity 0.25 $\mu M$; (10)) and Lyn were identified as ligands for Nef using this approach ((12) and unpublished data). Conversely, the binding affinities measured for the specific interactions that we have identified have been in the low micromolar range or better (10, 42), and unpublished data).

Despite the relatively high predicted likelihood of the 324 proteins included in the current study to encode functional SH3 ligand proteins, significant enrichment of SH3-displaying phages from the library was observed only for 44 of them (13.6%), and only for 19 (5.6%) a distinct preference for individual SH3 domains could be seen. Although it is not possible to know how many of the examined ORFs actually encode bona fide SH3 ligands, we can conclude that strong and distinctly selective partnerships are relatively rare among SH3-mediated human protein interactions. This conclusion is in agreement with the fact that the majority of SH3 interactions described in the literature are relatively weak. Indeed, it has been proposed that low affinity and modest to poor selectivity are characteristic features of SH3 binding (43). Thus, the specificity of the cellular processes that these interactions regulate may be provided mainly by other contributing factors that our SH3 library approach would miss, such as further cooperative contacts between the SH3-containing protein and its ligand, additional interacting proteins participating in the same multiprotein complex, as well as subcellular compartmentalization.

On the other hand, despite forming a minority, our current data show that SH3 interactions with a high affinity and specificity do exist at a reasonable frequency. Using a semiquantitative interaction assay we could establish submicromolar affinities and a remarkably high selectivity in binding even to closely related SH3 domains for the dominant SH3 phage library-discovered interactions that we examined. Thus, our data suggest that in some instances SH3 binding could also play a major role in determining protein interaction partnerships, and in driving the assembly of specific protein complexes in cells. Structural analyses of such robust SH3 interactions described earlier have shown that when compared with typical SH3-ligand complexes they involve extended target peptides or even more complex binding determinants within the ligand protein, which cover a larger surface on the cognate SH3 domains (Nef/Hck-SH3 (11), p47$^{hox}$/p67$^{hox}$-SH3 (44), PEP/Csk-SH3 (45); PAK/$\beta$PIX (46, 47), SLP-76/GADS-SH3 (37, 38), and EspF$_U$/IRTKS-SH3 (42)).

A similar complex mode of binding is likely to be the case also with many or most of the SH3 interactions identified in this study. Supporting this notion, the SH3 binding intensity of the linear target motifs examined on our peptide array failed almost completely to explain the SH3 binding selectivity observed for the corresponding native target proteins in the phage library screen. The strongest peptide binding signals did not predict SH3 partners selected by the host proteins of these peptides. By contrast, in some cases SH3 domains that were highly preferred by certain ligand proteins failed to show significant binding to any peptide derived from this protein, although the same peptides bound well to other SH3 domain probes.

When considering the relative SH3 binding selectivity of the arrayed peptides rather than absolute strength of binding a somewhat better overlap between the two data sets could be seen. The IRTKS- and CIN85-derived peptides not only bound strongly but were unusually selective for Eps8L1 SH3 and CrkL SH3 (1/2), respectively. Likewise, HCLS1 and SH2B1 that predominantly selected Lyn SH3 from the phage library both contained a peptide that showed strong binding only to Lyn (EDNEEPPALPPRTLEGLQ and DSMELLPPELPPRIPIEE, respectively). Moreover, the preference of ArgBP2 for CIN85 SH3 (1/3) in phage-display could be correlated with the presence of the peptide PPPLPTTPTPVPREPGRK in ArgBP2 that bound strongly only to CIN85 SH3 (1/3) and CMS SH3 (1/3), but poorly to all other SH3 domains used as probes. Despite the high technical quality of the peptide array, however, apart from these few examples the peptide binding data were not generally helpful in explaining the SH3 selectivity shown by the corresponding native proteins in phage display.

Thus, we conclude that the SH3 selectivity of the 19 native protein ligands examined in this study is either based on binding determinants that are located outside of the core SH3 binding motifs contained in the arrayed peptides, or alternatively, are dependent on a particular conformation of the peptide that is lost when it is no longer presented as a part of the corresponding folded protein. In either case, our data suggest that large-scale peptide arrays screens have relatively limited value for attempts to characterize relevant SH3-mediated protein interaction networks in cells.

It is pertinent to compare our current approach to the previously reported SH3 interactome studies that have been based on large-scale Y2H combined with extensive peptide library screens (30, 31, 33). These authors concluded that Y2H and peptide array screens query different but overlapping regions of protein-protein interaction (PPI) space. Mapping of the SH3 interactome using Y2H resembles our approach in that it involves the use of folded ligand proteins rather than short target peptides. On the other, it differs from our phage display screening approach in involving more confounding biological variables other than binding affinity, and thereby may also identify weak or false interactions as "hits." It has been suggested that the predictive value of such large-scale screens could be increased by integrating the data from Y2H

and peptide array screens, *i.e.* considering only interactions indicated by both approaches. However, in light of our current data, ignoring strong SH3-protein interactions that are not matched by a strong SH3-peptide interaction would not seem like a good strategy. Such filtering would probably bias the results toward a subpopulation of interactions that involve atypical peptide binding motifs (such as the IRTKS - Eps8L1/3 interaction identified here), but would miss all interactions that are strong and selective despite involving a typical low-affinity SH3 binding core motif.

As already noted above, our SH3 phage display screening approach involves a relatively high affinity threshold for interaction identification. Because it also involves competition for ligand binding by an essentially complete repertoire of human SH3 domains it is indeed well suited for discovery of strong and selective SH3 interactions. Although it is logical to assume that such interactions have a high likelihood of being relevant, it is also clear that this kind of a binding profile alone does not establish biological significance. On the other hand, it is important to note that the reverse is also true, and lack of high binding affinity and apparent specificity of an SH3/ligand interaction studied in isolation do not exclude a major role in cellular regulation. In any case, the strong and selective interactions identified here using 324 predicted SH3 ligand proteins provide a valuable collection of novel interactions that may regulate cell behavior and potentially reveal new targets for therapeutic development. In Table II 57 such interactions involving 19 different target proteins are listed, most of which represent interactions that have not been described before. Several of these suggest interesting and readily testable hypotheses of potential medical importance.

For example, a novel regulatory circuit operative in reactive oxygen species (ROS) production and neutrophil phagosome function that is relevant to pathogen defenses and chronic granulomatous disease (see (48)) is suggested by the interactions between the second (of three) SH3 domains of Ponsin and ArgBP2 with the NCF1 (p47-phox) and NCF2 (p67-phox) regulatory subunits of the NOX2 neutrophil NADPH oxidase complex. Ponsin (SORBS1) and ArgBP2 (SORBS2) are signaling factors that together with vinexin (SORBS3) form the SoHo family of adapter proteins (49). Our previous SH3 interaction screens have revealed binding of the third SH3 of the SoHo proteins to the p21-activated kinase (PAK) (12), an interaction that is also independently supported by cell biology studies (50). Because PAK acts as an activator of NADPH oxidase complex and ROS production by phosphorylating NCF1 (51), our studies suggest an important role for the ArgBP2 and ponsin adapter proteins as signaling platforms that coordinate NADPH oxidase complex activation via their dual capacity to bind NADPH subunits (via SH3 (2/3)) and PAK (via SH3 (3/3)). In support of this possibility, we have observed that NOX2-mediated ROS production is inhibited in cells overexpressing an ArgBP2 variant carrying an inactivating mutation in its third SH3 domain (unpublished data).

Further characterization of biological significance of the novel SH3 interactions revealed in our screen is clearly warranted. Also, despite the relatively low "hit rate" in this study, extension of the current study to even higher numbers of potential human ligands predicted by algorithms similar those used here as well as modified ones would seem like a worthwhile endeavor. However, in order to achieve the goal of comprehensive characterization of the human SH3 interactome, novel high-throughput methods based on functional read-outs rather than affinity ranking of SH3-ligand interactions will also be needed.

Ⓢ This article contains supplemental material.

¶ To whom correspondence should be addressed: Department of Virology, University of Helsinki, PO Box 21 (Haartmaninkatu 3) 00014-University of Helsinki, Finland. Tel.: +358 2 9412 6770; Fax: +358 2 9412 6491; E-mail: kalle.saksela@helsinki.fi.

‖ These authors contributed equally to this study.

** Current address: Laboratory of Neurooncology and Genetics, Neuroscience Institute, Lithuanian University of Health Sciences, Kaunas, Lithuania.

## REFERENCES

1. Mayer, B. J., and Saksela, K. (2005) SH3 domains. In: Cesareni, G., Gimona, M., Sudol, M., and Yaffe, M., ed. *Modular Protein Domains*, pp. 37–58, Wiley-VCH, Weinheim
2. Mayer, B. J., and Gupta, R. (1998) Functions of SH2 and SH3 domains. *Curr. Top. Microbiol. Immunol.* **228,** 1–22
3. Pawson, T. (1994) SH2 and SH3 domains in signal transduction. *Adv. Cancer Res.* **64,** 87–110
4. Bliska, J. (1996) How pathogens exploit interactions mediated by SH3 domains. *Chem. Biol.* **3,** 7–11
5. Davey, N. E., Trave, G., and Gibson, T. J. (2011) How viruses hijack cell regulation. *Trends Biochem. Sci.* **36,** 159–169
6. Saksela, K. (2011) Interactions of the HIV/SIV pathogenicity factor Nef with SH3 domain-containing host cell proteins. *Curr. HIV Res.* **9,** 531–542
7. Kaneko, T., Sidhu, S. S., and Li, S. S. (2011) Evolving specificity from variability for protein interaction domains. *Trends Biochem. Sci.* **36,** 183–190
8. Mayer, B. J. (2001) SH3 domains: complexity in moderation. *J. Cell Sci.* **114,** 1253–1263
9. Saksela, K., and Permi, P. (2012) SH3 domain ligand binding: What's the consensus and where's the specificity? *FEBS Lett.* **586,** 2609–2614
10. Lee, C. H., Leung, B., Lemmon, M. A., Zheng, J., Cowburn, D., Kuriyan, J., and Saksela, K. (1995) A single amino acid in the SH3 domain of Hck determines its high affinity and specificity in binding to HIV-1 Nef protein. *EMBO J.* **14,** 5006–5015
11. Lee, C. H., Saksela, K., Mirza, U. A., Chait, B. T., and Kuriyan, J. (1996) Crystal structure of the conserved core of HIV-1 Nef complexed with a Src family SH3 domain. *Cell* **85,** 931–942
12. Kärkkäinen, S., Hiipakka, M., Wang, J. H., Kleino, I., Vähä-Jaakkola, M., Renkema, G. H., Liss, M., Wagner, R., and Saksela, K. (2006) Identification of preferred protein interactions by phage-display of the human Src homology-3 proteome. *EMBO Rep.* **7,** 186–191
13. Asbach, B., Ludwig, C., Saksela, K., and Wagner, R. (2012) Comprehensive analysis of interactions between the Src-associated protein in mitosis of 68 kDa and the human Src-homology 3 proteome. *PLoS ONE* **7,** e38540

14. Kesti, T., Ruppelt, A., Wang, J. H., Liss, M., Wagner, R., Tasken, K., and Saksela, K. (2007) Reciprocal regulation of SH3 and SH2 domain binding via tyrosine phosphorylation of a common site in CD3epsilon. *J. Immunol.* **179,** 878–885

15. Kleino, I., Ortiz, R. M., Yritys, M., Huovila, A. P., and Saksela, K. (2009) Alternative splicing of ADAM15 regulates its interactions with cellular SH3 proteins. *J. Cell. Biochem.* **108,** 877–885

16. Neuvonen, M., Kazlauskas, A., Martikainen, M., Hinkkanen, A., Ahola, T., and Saksela, K. (2011) SH3 domain-mediated recruitment of host cell amphiphysins by alphavirus nsP3 promotes viral RNA replication. *PLoS Pathog.* **7,** e1002383

17. Pietrek, M., Brinkmann, M. M., Glowacka, I., Enlund, A., Havemeier, A., Dittrich-Breiholz, O., Kracht, M., Lewitzky, M., Saksela, K., Feller, S. M., and Schulz, T. F. (2010) Role of the Kaposi's sarcoma-associated herpesvirus K15 SH3 binding site in inflammatory signaling and B-cell activation. *J. Virol.* **84,** 8231–8240

18. Vingadassalom, D., Kazlauskas, A., Skehan, B., Cheng, H. C., Magoun, L., Robbins, D., Rosen, M. K., Saksela, K., and Leong, J. M. (2009) Insulin receptor tyrosine kinase substrate links the E. coli O157:H7 actin assembly effectors Tir and EspF(U) during pedestal formation. *Proc. Natl. Acad. Sci. U.S.A.* **106,** 6754–6759

19. Heikkinen, L. S., Kazlauskas, A., Melen, K., Wagner, R., Ziegler, T., Julkunen, I., and Saksela, K. (2008) Avian and 1918 Spanish influenza a virus NS1 proteins bind to Crk/CrkL Src homology 3 domains to activate host cell signaling. *J. Biol. Chem.* **283,** 5719–5727

20. Schmaier, A. A., Zou, Z., Kazlauskas, A., Emert-Sedlak, L., Fong, K. P., Neeves, K. B., Maloney, S. F., Diamond, S. L., Kunapuli, S. P., Ware, J., Brass, L. F., Smithgall, T. E., Saksela, K., and Kahn, M. L. (2009) Molecular priming of Lyn by GPVI enables an immune receptor to adopt a hemostatic role. *Proc. Natl. Acad. Sci. U.S.A.* **106,** 21167–21172

21. Antoku, S., Saksela, K., Rivera, G. M., and Mayer, B. J. (2008) A crucial role in cell spreading for the interaction of Abl PxxP motifs with Crk and Nck adaptors. *J. Cell Sci.* **121,** 3071–3082

22. Thompson, O., Kleino, I., Crimaldi, L., Gimona, M., Saksela, K., and Winder, S. J. (2008) Dystroglycan, Tks5 and Src mediated assembly of podosomes in myoblasts. *PLoS ONE* **3,** e3638

23. Amako, Y., Igloi, Z., Mankouri, J., Kazlauskas, A., Saksela, K., Dallas, M., Peers, C., and Harris, M. (2013) Hepatitis C virus NS5A inhibits mixed lineage kinase 3 to block apoptosis. *J. Biol. Chem.* **288,** 24753–24763

24. Igloi, Z., Kazlauskas, A., Saksela, K., Macdonald, A., Mankouri, J., and Harris, M. (2015) Hepatitis C virus NS5A protein blocks epidermal growth factor receptor degradation via a proline motif- dependent interaction. *J. Gen. Virol.* **96,** 2133–2144

25. Kleino, I., Jarviluoma, A., Hepojoki, J., Huovila, A. P., and Saksela, K. (2015) Preferred SH3 domain partners of ADAM metalloproteases include shared and ADAM-specific SH3 interactions. *PLoS ONE* **10,** e0121301

26. Brannetti, B., Via, A., Cestra, G., Cesareni, G., and Helmer-Citterich, M. (2000) SH3-SPOT: an algorithm to predict preferred ligands to different members of the SH3 gene family. *J. Mol. Biol.* **298,** 313–328

27. Carducci, M., Perfetto, L., Briganti, L., Paoluzi, S., Costa, S., Zerweck, J., Schutkowski, M., Castagnoli, L., and Cesareni, G. (2012) The protein interaction network mediated by human SH3 domains. *Biotechnol. Adv.* **30,** 4–15

28. Landgraf, C., Panni, S., Montecchi-Palazzi, L., Castagnoli, L., Schneider-Mergener, J., Volkmer-Engert, R., and Cesareni, G. (2004) Protein interaction networks by proteome peptide scanning. *PLos Biol.* **2,** E14

29. Liu, B. A., Engelmann, B. W., and Nash, P. D. (2012) High-throughput analysis of peptide-binding modules. *Proteomics* **12,** 1527–1546

30. Tong, A. H., Drees, B., Nardelli, G., Bader, G. D., Brannetti, B., Castagnoli, L., Evangelista, M., Ferracuti, S., Nelson, B., Paoluzi, S., Quondam, M., Zucconi, A., Hogue, C. W., Fields, S., Boone, C., and Cesareni, G. (2002) A combined experimental and computational strategy to define protein interaction networks for peptide recognition modules. *Science* **295,** 321–324

31. Tonikian, R., Xin, X., Toret, C. P., Gfeller, D., Landgraf, C., Panni, S., Paoluzi, S., Castagnoli, L., Currell, B., Seshagiri, S., Yu, H., Winsor, B., Vidal, M., Gerstein, M. B., Bader, G. D., Volkmer, R., Cesareni, G., Drubin, D. G., Kim, P. M., Sidhu, S. S., and Boone, C. (2009) Bayesian modeling of the yeast SH3 domain interactome predicts spatiotemporal dynamics of endocytosis proteins. *PLos Biol.* **7,** e1000218

32. Wu, C., Ma, M. H., Brown, K. R., Geisler, M., Li, L., Tzeng, E., Jia, C. Y., Jurisica, I., and Li, S. S. (2007) Systematic identification of SH3 domain-mediated human protein-protein interactions by peptide array target screening. *Proteomics* **7,** 1775–1785

33. Xin, X., Gfeller, D., Cheng, J., Tonikian, R., Sun, L., Guo, A., Lopez, L., Pavlenco, A., Akintobi, A., Zhang, Y., Rual, J. F., Currell, B., Seshagiri, S., Hao, T., Yang, X., Shen, Y. A., Salehi-Ashtiani, K., Li, J., Cheng, A. T., Bouamalay, D., Lugari, A., Hill, D. E., Grimes, M. L., Drubin, D. G., Grant, B. D., Vidal, M., Boone, C., Sidhu, S. S., and Bader, G. D. (2013) SH3 interactome conserves general function over specific form. *Mol. Syst. Biol.* **9,** 652

34. Lamesch, P., Li, N., Milstein, S., Fan, C., Hao, T., Szabo, G., Hu, Z., Venkatesan, K., Bethel, G., Martin, P., Rogers, J., Lawlor, S., McLaren, S., Dricot, A., Borick, H., Cusick, M. E., Vandenhaute, J., Dunham, I., Hill, D. E., and Vidal, M. (2007) hORFeome v3.1: a resource of human open reading frames representing over 10,000 human genes. *Genomics* **89,** 307–315

35. Rual, J. F., Hill, D. E., and Vidal, M. (2004) ORFeome projects: gateway between genomics and omics. *Curr. Opinion Chem. Biol.* **8,** 20–25

36. Frank, R. (2002) The SPOT-synthesis technique. Synthetic peptide arrays on membrane supports–principles and applications. *J. Immunol. Methods* **267,** 13–26

37. Harkiolaki, M., Lewitzky, M., Gilbert, R. J., Jones, E. Y., Bourette, R. P., Mouchiroud, G., Sondermann, H., Moarefi, I., and Feller, S. M. (2003) Structural basis for SH3 domain-mediated high-affinity binding between Mona/Gads and SLP-76. *EMBO J.* **22,** 2571–2582

38. Liu, Q., Berry, D., Nash, P., Pawson, T., McGlade, C. J., and Li, S. S. (2003) Structural basis for specific binding of the Gads SH3 domain to an RxxK motif-containing SLP-76 peptide: a novel mode of peptide recognition. *Mol. Cell* **11,** 471–481

39. Takemoto, Y., Sato, M., Furuta, M., and Hashimoto, Y. (1996) Distinct binding patterns of HS1 to the Src SH2 and SH3 domains reflect possible mechanisms of recruitment and activation of downstream molecules. *Int. Immunol.* **8,** 1699–1705

40. Rickles, R. J., Botfield, M. C., Weng, Z., Taylor, J. A., Green, O. M., Brugge, J. S., and Zoller, M. J. (1994) Identification of Src, Fyn, Lyn, PI3K and Abl SH3 domain ligands using phage display libraries. *EMBO J.* **13,** 5598–5604

41. Arold, S., O'Brien, R., Franken, P., Strub, M. P., Hoh, F., Dumas, C., and Ladbury, J. E. (1998) RT loop flexibility enhances the specificity of Src family SH3 domains for HIV-1 Nef. *Biochemistry* **37,** 14683–14691

42. Aitio, O., Hellman, M., Kazlauskas, A., Vingadassalom, D. F., Leong, J. M., Saksela, K., and Permi, P. (2010) Recognition of tandem PxxP motifs as a unique Src homology 3-binding mode triggers pathogen-driven actin assembly. *Proc. Natl. Acad. Sci. U.S.A.* **107,** 21743–21748

43. Ladbury, J. E., and Arold, S. (2000) Searching for specificity in SH domains. *Chem Biol* **7,** R3–R8

44. Kami, K., Takeya, R., Sumimoto, H., and Kohda, D. (2002) Diverse recognition of non-PxxP peptide ligands by the SH3 domains from p67(phox), Grb2 and Pex13p. *EMBO J.* **21,** 4268–4276

45. Ghose, R., Shekhtman, A., Goger, M. J., Ji, H., and Cowburn, D. (2001) A novel, specific interaction involving the Csk SH3 domain and its natural ligand. *Nat. Struct. Biol.* **8,** 998–1004

46. Hoelz, A., Janz, J. M., Lawrie, S. D., Corwin, B., Lee, A., and Sakmar, T. P. (2006) Crystal structure of the SH3 domain of betaPIX in complex with a high affinity peptide from PAK2. *J. Mol. Biol.* **358,** 509–522

47. Mott, H. R., Nietlispach, D., Evetts, K. A., and Owen, D. (2005) Structural analysis of the SH3 domain of beta-PIX and its interaction with alpha-p21 activated kinase (PAK). *Biochemistry* **44,** 10977–10983

48. Segal, B. H., Grimm, M. J., Khan, A. N., Han, W., and Blackwell, T. S. (2012) Regulation of innate immunity by NADPH oxidase. *Free Radical Biol. Med.* **53,** 72–80

49. Roignot, J., and Soubeyran, P. (2009) ArgBP2 and the SoHo family of adapter proteins in oncogenic diseases. *Cell Adhesion Migration* **3,** 167–170

50. Yuan, Z. Q., Kim, D., Kaneko, S., Sussman, M., Bokoch, G. M., Kruh, G. D., Nicosia, S. V., Testa, J. R., and Cheng, J. Q. (2005) ArgBP2gamma interacts with Akt and p21-activated kinase-1 and promotes cell survival. *J. Biol. Chem.* **280,** 21483–21490

51. Martyn, K. D., Kim, M. J., Quinn, M. T., Dinauer, M. C., and Knaus, U. G. (2005) p21-activated kinase (Pak) regulates NADPH oxidase activation in human neutrophils. *Blood* **106,** 3962–3969